The Spine Journal 19 (2019) 1584–1596

Basic Science

Differential miRNAs profile and bioinformatics analyses in bone marrow mesenchymal stem cells from adolescent idiopathic scoliosis patients

Shangyi Hui, MD[a,#], Yang Yang, MD[b,#], Jing Li, MD[c], Na Li, MD[c], Pengchao Xu, MD[c], Hongling Li, MD[c], Yanbin Zhang, MD[b], Shengru Wang, MD[b], Guanfeng Lin, MD[b], Shugang Li, MD[b], Guixing Qiu, MD[b], Robert Chunhua Zhao, MD[c], Jianguo Zhang, MD[b,†], Qianyu Zhuang, MD[b,†,*]

[a] *Department of Anesthesiology, Peking Union Medical College Hospital, Beijing, PR China*
[b] *Department of Orthopedics, Peking Union Medical College Hospital, Beijing, PR China*
[c] *Center of Excellence in Tissue Engineering, Institute of Basic Medical Sciences and School of Basic Medicine, Chinese Academy of Medical Sciences and Peking Union Medical College, Beijing Key Laboratory of New Drug Development and Clinical Trial of Stem Cell Therapy, Beijing, PR China*

Received 27 November 2018; revised 7 May 2019; accepted 7 May 2019

Abstract

BACKGROUND CONTEXT: Coexistence of abnormal skeletal growth and reduced bone mineral density in the context of adolescent idiopathic scoliosis (AIS) suggests disturbed bone metabolism existing in such patients. Our previous study suggested increased proliferation ability and decreased osteogenic differentiation ability of bone marrow mesenchymal stem cells (BM-MSCs) of AIS.

PURPOSE: To explore the differential miRNA expression profile, Go (gene ontology) terms and KEGG (Kyoto Encyclopedia of Genes and Genomes) pathways in BM-MSCs of AIS and non-AIS controls were conducted using microarray approach and bioinformatics analyses.

STUDY DESIGN: miRNA microarray approach and bioinformatics analysis.

METHODS: The differentially expressed miRNAs (DEMs) of BM-MSCs from AIS patients compared with those from healthy individuals were analyzed using a microarray analysis. Comprehensive bioinformatics analyses were then used to enrich datasets for gene ontology and pathway. Based on the interaction network analysis of DEMs contained in significant pathways, 12 potential crucial miRNAs were selected for validation by RT-PCR.

RESULTS: The study identified 54 previously unrecognized DEMs (12 upregulated, 42 downregulated) in BM-MSCs from AIS patients. These miRNAs are involved in multiple biological processes, including small GTPase-mediated signal transduction, DNA-dependent transcription, cytokinesis, cell adhesion, transmembrane transport, response to hypoxia, etc. Pathway analysis of these new identified miRNAs revealed dysregulated MAPK signaling pathway, PI3K-Akt signaling pathway, calcium signaling pathway, Notch signaling pathway, and ubiquitin-mediated proteolysis pathway, all of which have been reported to play important role in regulating the osteogenic or adipogenic differentiation of MSCs. Furthermore, interaction networks analysis indicated that seven most significant central miRNAs, including miR-17-5p, miR-106a-5p, miR-106b-5p, miR-16-5p,

FDA device/drug status: Not applicable.

Author disclosures: ***SH***: Nothing to disclose. ***YY***: Nothing to disclose. ***JL***: Nothing to disclose. ***NL***: Nothing to disclose. ***PX***: Nothing to disclose. ***HL***: Nothing to disclose. ***YZ***: Nothing to disclose. ***SW***: Nothing to disclose. ***GL***: Nothing to disclose. ***SL***: Nothing to disclose. ***GQ***: Nothing to disclose. ***RCZ***: Nothing to disclose. ***JZ***: Grants: National Natural Science Foundation of China (E). ***QZ***: Grants: National Natural Science Foundation of China (E); Beijing Talent Fund (B); Beijing Nova program Grant (B); Peking Union Medical College Youth Fund (B); PUMC Nova program Grant of Chinese academy of medical sciences (B); Beijing High-level Innovative Entrepreneurial Talent Fund (C).

* Corresponding author: Peking Union Medical College Hospital, 1 Shuai Fu Yuan, Beijing 100730, PR China. Tel.: 86-13552869326; fax: 86-10-69152809.

E-mail address: zhuangqianyu@hotmail.com (Q. Zhuang).

# These two authors contribute equally to this paper as the first authors.

† These authors contribute equally to this paper as the corresponding authors.

https://doi.org/10.1016/j.spinee.2019.05.003

miR-93-5p, miR-15a-5p, and miR-181b-5p may play essential roles in AIS pathogenesis and accompanied osteopenia.

CONCLUSION: The current study reports the differential miRNAs expression profiles of BM-MSCs from AIS patients and related pathways for the first time. The identification of these candidate miRNAs provides a deep insight into the pathogenesis of AIS and the accompanying generalized osteopenia.

Keywords: Adolescent idiopathic scoliosis; bone marrow mesenchymal stem cells; osteopenia; microarray; Differentially expressed miRNA; pathway.

Introduction

Coexistence of abnormal skeletal growth [1−3] and reduced bone mineral density [4−6] in the context of adolescent idiopathic scoliosis (AIS) suggests disturbed bone metabolism existing in such patients [7,8]. Mesenchymal stem cells (MSCs), with the inherent osteoblastogenic and adipogenic potentialities, have been reported to play a crucial role in bone mass homeostasis in AIS [9−12]. While research interests have been devoted to the genetic analysis of MSCs in AIS patients [10−12], regulation of the genetic pathogenesis remains yet to be discerned.

MicroRNAs (miRNAs) have been reported as extensively involved in regulating osteoblastic and osteoclastic functions [13−15]. Despite that the regulatory role of miRNAs has been well established in human bone cells, exploratory studies on miRNA functionality in MSCs of AIS patients are still scarce.

In previous studies, the authors have reported the differential genetic and proteomic expression levels in MSCs obtained from AIS patients [11,16]. In this study, the authors adopted a microarray approach to investigate the miRNA expression profiles in MSCs of AIS patients. The miRNA expression profiles were further processed using gene ontology (GO), Kyoto Encyclopedia of Genes and Genomes (KEGG) orthology, and miRNA target gene & pathway network, with the expectations of exploring potentially crucial miRNAs involved in the pathogenesis of AIS and the accompanying generalized osteopenia through comprehensive bioinformatic analyses.

Materials and methods

Patients and specimens

Bone marrow (BM) aspirates were obtained from 10 AIS patients and 5 non-AIS patients with lower-leg fracture (Table 1), as previously described [11]. In the AIS group, 10 patients, with a mean age of 13.6 years old (ranging from 1"2 to 16 years old), underwent full clinical and radiological examinations (X-ray, CT, and MRI) to rule out other causes of scoliosis and to ascertain the diagnosis of AIS. The subject exclusion criteria were scoliosis of congenital, neuromuscular, or metabolic etiology, skeletal dysplasia, known endocrine and connective tissue abnormalities, and mental retardation. CT and MRI are used to exclude congenital vertebral malformation and intraspinal pathologies (syringomyelia, diastematomyelia, tether cord, etc.). In the control group, five age- and sex-matched subjects, with a mean age of 13.8 years old (ranging from 12 to 16 years old), all had a straight spine and a normal forward bending test on the physical examination. They were confirmed to be free of any associated medical diseases or spinal deformities when entered to the study. The study was approved by the Ethics Committee of Peking Union Medical College Hospital. Written informed consents were obtained from all subjects and their parents before entering the study.

Cell culture and differentiation of BM-MSCs

As described in our previous study [11], BM-MSCs were isolated using the same techniques, and confluent cells

Table 1
Clinical characteristics of AIS patients

Patient	Gender	Age at diagnosis	Lenke classification [24]	PUMC classification [25]	Location of major curve	Cobb's angle	Apical vertebra	Spinal surgery	Bracing
1	Female	13	1CN	ⅡC	Right thoracic/left lumbar	41˚/37˚	T8/L2	Yes	Yes
2	Male	13	5CN	ⅡC	Right thoracic/left lumbar	35˚/65˚	T8/L2	Yes	Yes
3	Female	13	1B-	ⅠA	Right thoracic	40˚	T8	Yes	Yes
4	Female	12	1BN	ⅠA	Right thoracic	44˚	T8	Yes	Yes
5	Female	13	1B-	ⅡB1	Right thoracic/left lumbar	41˚/15˚	T8/L2	Yes	Yes
6	Male	13	1CN	ⅢA	Left PT/right MT/left lumbar	29˚/53˚/36˚	T2/ T8/L2	Yes	Yes
7	Female	13	5CN	ⅡD1	Right thoracic/left lumbar	20˚/40˚	T8/L1	Yes	Yes
8	Female	16	1BN	ⅡB1	Right thoracic/left lumbar	44˚/34˚	T9/L3	Yes	No
9	Male	15	1B-	ⅡA1	Right PT/left MT	29˚/46˚	T2/T8	Yes	No
10	Female	15	1BN	ⅡD2	Right thoracic	60˚	T9	Yes	Yes

The table presents characteristics of 10 patients with AIS who were selected based upon described criteria.

Table 2
RT-qPCR primers sequences for seven validated miRNAs

Gene name	Primer sequence
hsa-miR-17-5p	CAAAGTGCTTACAGTGCAGGTAG
hsa-miR-106a-5p	AAAAGTGCTTACAGTGCAGGTAG
hsa-miR-106b-5p	TAAAGTGCTGACAGTGCAGAT
hsa-miR-16-5p	TAGCAGCACGTAAATATTGGCG
hsa-miR-93-5p	CAAAGTGCTGTTCGTGCAGGTAG
hsa-miR-15a-5p	TAGCAGCACATAATGGTTTGTG
hsa-miR-181b-5p	AACATTCATTGCTGTCGGTGGGT

(approximately 2×10^6) at the third passage were used for the following experiments. Primary antibodies against human CD29, CD31, CD34, CD44, CD45, CD73, and CD105 (BD Biosciences) were used for immunophenotype analysis of BM-MSCs.

MSCs were cultured under differentiation conditions. As previously described [11], cells were stained with the ALP staining kit (Beyotime, China) to reveal osteogenic differentiation and stained with fresh Oil Red O solution (Sigma,

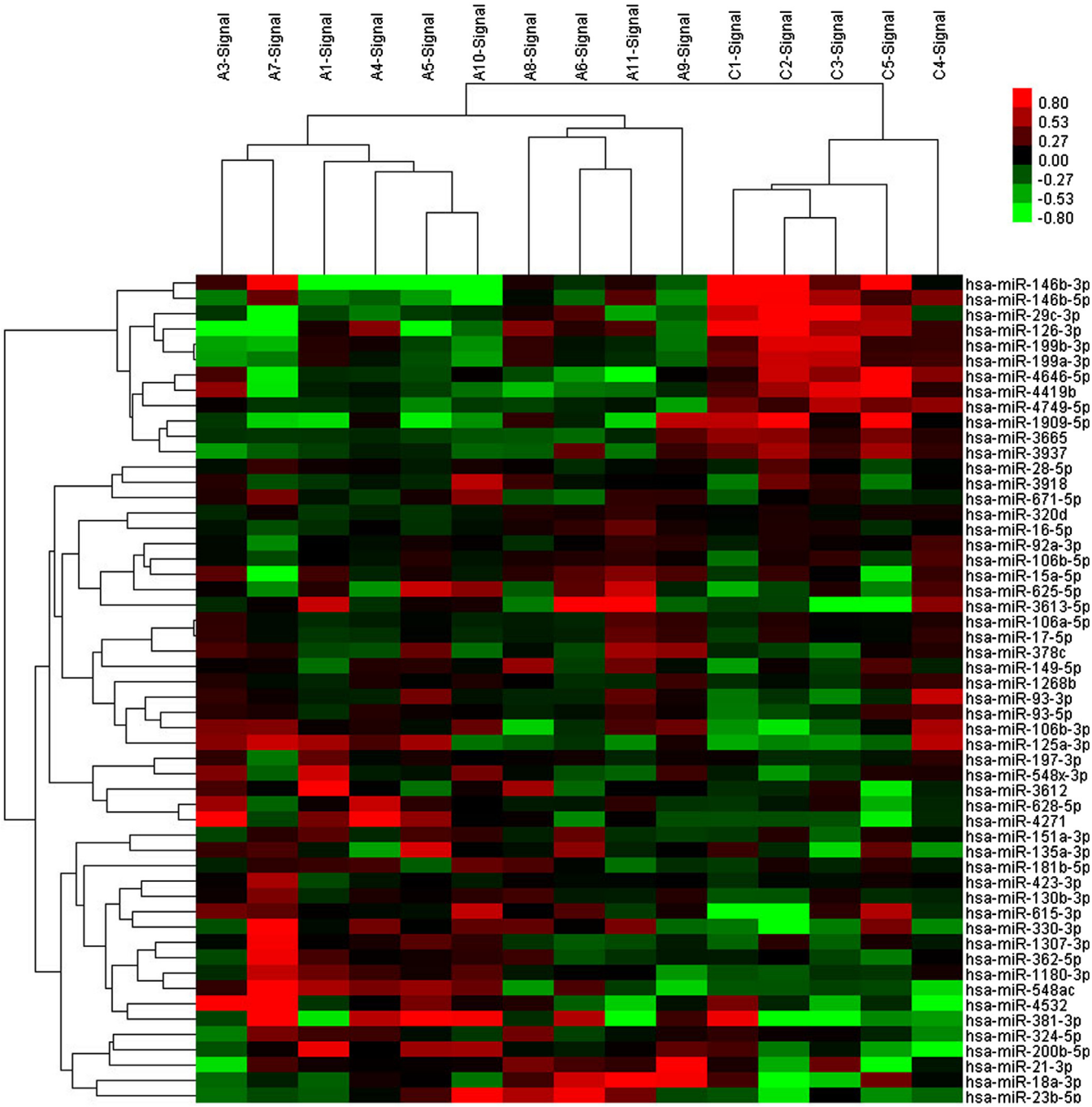

Fig. 1. Clustering analysis for the selected differentially expressed miRNAs. The horizontal axis represents the samples, and the left vertical axis represents the genes (pink bar: downregulated miRNAs; orange: upregulated miRNAs). Red and green represents upregulation and downregulation separately.

St. Louis, MO) to show lipid droplets in adipogenic differentiation-induced cells.

Total RNA extraction and microarray assay

RNA was extracted from MSCs using TRIzol Reagent (Invitrogen, Carlsbad, CA). Following purification with a RNeasy kit (Qiagen, Valencia, CA), cDNA was generated using One-Cycle Target Labeling and Control Reagents (Affymetrix, Santa Clara, CA), and cRNA was created with a GeneChip WT Labeling Kit (Affymetrix, Santa Clara, CA). Biotin-labeled, fragmented (200 nt) cRNA was then hybridized for 16 hours at 45°C Affymetrix GeneChip HumanTranscript 2.0 arrays (Affymetrix). GeneChips were washed and stained in the Affymetrix Fluidics Station 450. GeneChips were scanned by using Affymetrix GeneChip Command Console (AGCC) which installed in GeneChip Scanner 3000 7G. The data were analyzed with robust multichip analysis algorithm using Affymetrix default analysis settings and global scaling as normalization method. Values presented are log2 robust multichip analysis signal intensity.

Differentially expressed miRNAs were identified based on random-variance model *t* test and false discovery rate (FDR) analysis. $p<.05$ and $FDR<0.05$ was set as a threshold. Cluster 3.0 and TreeView analysis (Stanford University, California, USA) were performed to generate a dendrogram for each cluster of genes based on their expression profiling similarities.

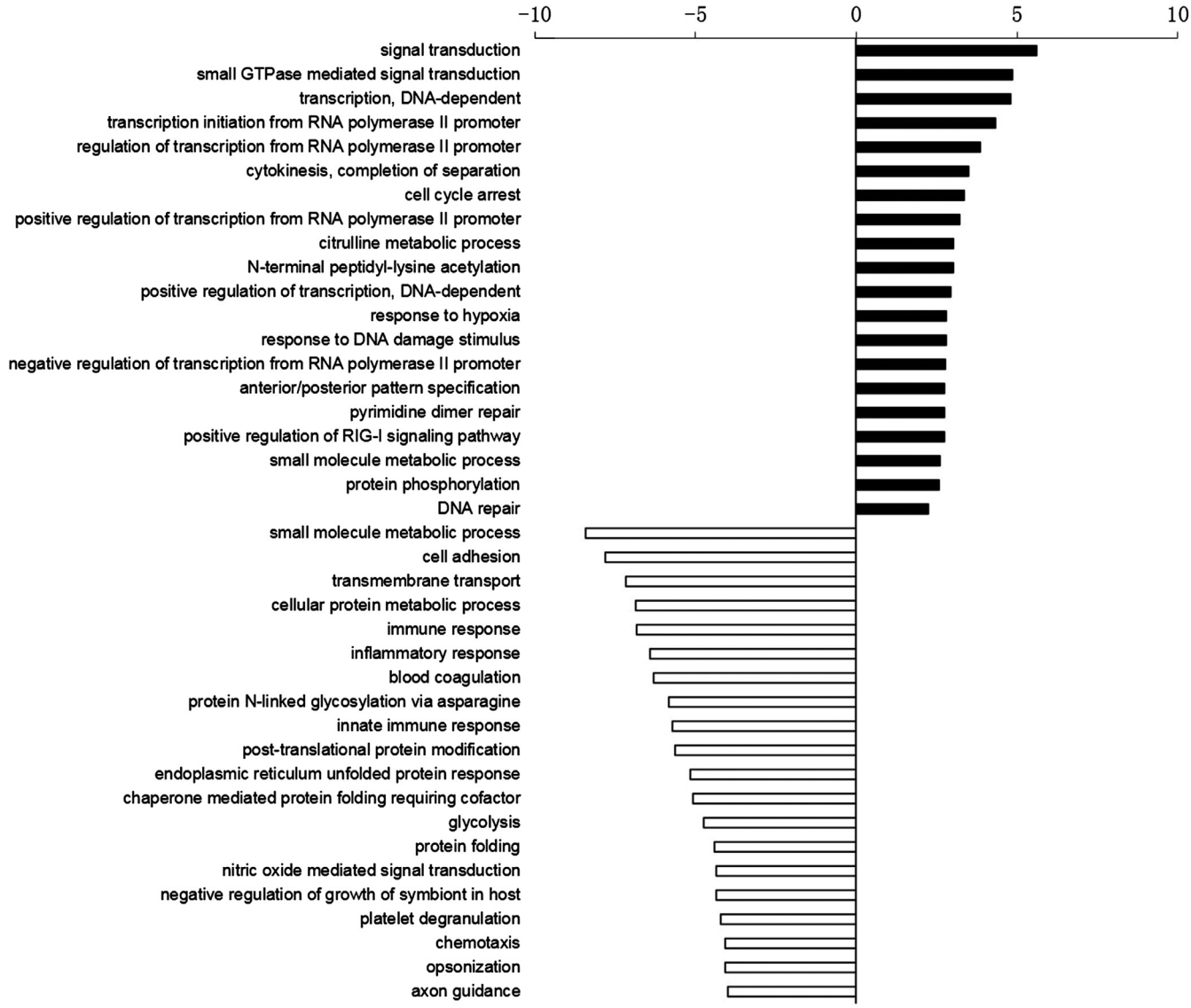

Fig. 2. The significant GO categories of the target genes. The figure shows significant GO categories targeted by upregulated and downregulated categories, respectively. The vertical axis is the gene ontology category, and the horizontal axis is the −lg p of GO categories (only shown when lg p>2, LgP is the logarithm of p value).

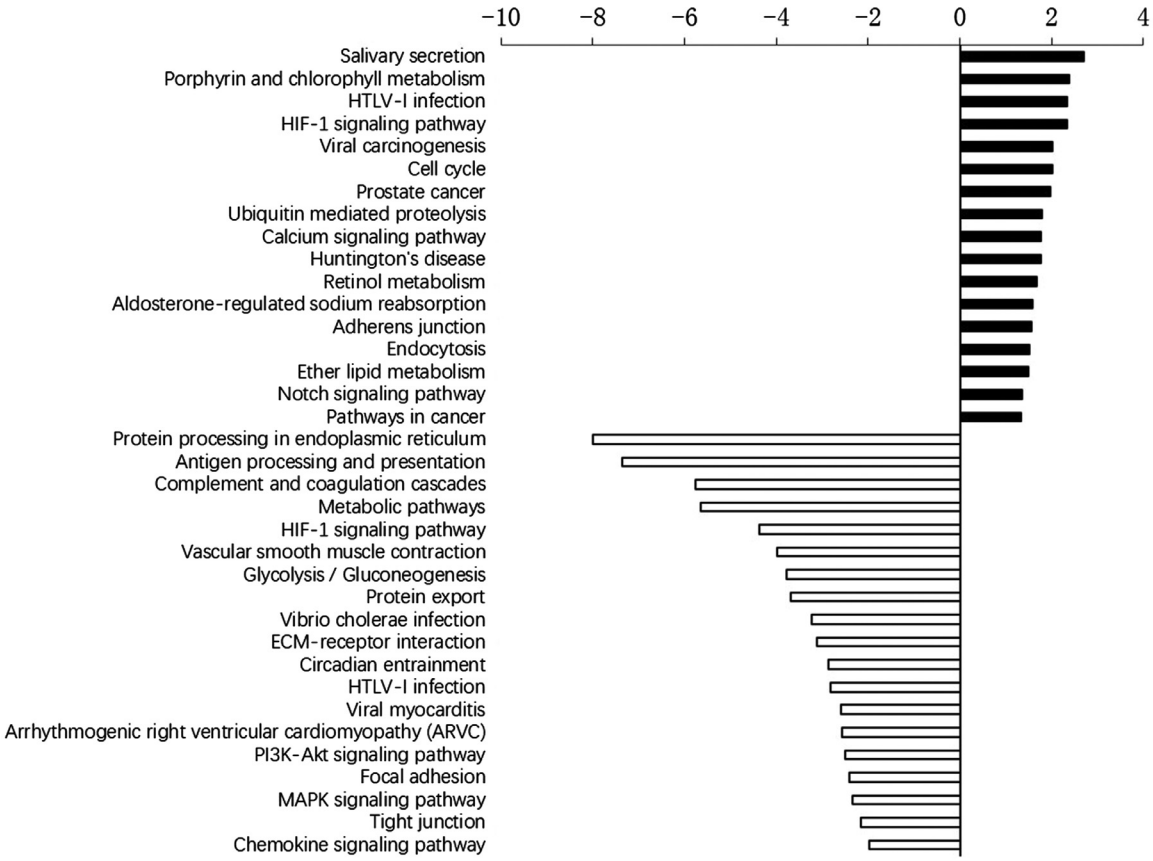

Fig. 3. The significant pathways of target genes. The figure shows significant pathways targeted by upregulated and downregulated pathways, respectively. The vertical axis is the pathway category, and the horizontal axis is the −lg p of pathways.

GO and pathway analysis

Functional analysis of differentially expressed miRNAs was carried out by the GO project (http://www.geneontology.org) on the basis of biological process, while pathway analysis was used to find out the significant pathway of the differential miRNAs according to KEGG (http://www.genome.jp/kegg/). The Fisher exact test and χ^2 test were used to classify the GO category and pathway, and the FDR was calculated to correct the p value. $p<.05$ and $FDR<0.1$ were used as a threshold to select significant GO categories and pathways.

MiRNA target gene, miRNA target GO, and miRNA target pathway network analysis

MiRNA target gene, miRNA target GO, and miRNA target pathway analysis were constructed based on the data of differential expressed miRNAs and target genes, target GOs, and target pathways. The networks for each miRNA were measured by counting the number of target genes and target GOs or target pathways, which were shown as degree respectively. A higher degree indicated that a miRNA regulated more genes, more GOs, more pathways, implying a more important role in the network. Venn diagram of the overlap top 10 miRNAs with the highest degree was established based on these three networks to investigate the most significant central miRNAs.

Extended sample validation of microarray data by real-time PCR

Based on the results of the Venn diagram of the overlap top 10 miRNAs of the three networks, a total of seven potentially crucial miRNAs were selected for validation. Total RNA was isolated from the third passage of BM-MSCs from 30 AIS patients and 20 controls. RNA was reverse transcribed using ReverTra Ace qPCR RT Kit (TOYOBO, Osaka, Japan). Quantitative real-time reverse transcription polymerase chain reaction (qRT-PCR) was conducted in a 20 μL reaction system consisting of 10 μL SYBR Green Real-time PCR MasterMix, 1 μL 10 mM forward primers, 1μL 10 mM reverse primers (listed in Table 2), 1 μL template cDNA, and 7 μL double-distilled water. The PCR cycling programs began with an initial denaturation for 5 minutes at 94°C, followed by 40 cycles of 30 seconds at 94°C, 30 seconds at 60°C to 65°C, 30 seconds at 72°C, and ended with the step of melting curve. The relative changes in gene expression were calculated by $2^{-\triangle\triangle Ct}$ method. U6 RNA was used as internal control to normalize the expression level.

Statistical analysis

The lists of miRNAs were extracted based on statistical test p values (<.05 was considered significant). The representatives of replicate experiments were shown in the figures and the data were shown as the means±SD. The statistical analyses were performed using independent Student's *t* tests.

Results

Culture and identification of MSCs

The cultured cells were all displayed classic fibroblast-like morphology under a light microscope. In immunophenotype analysis, these cells were persistently negative for CD31, CD34, and CD45, but positive for CD29, CD44, CD73, and CD105 (Supplementary Fig. 1), which suggested these cells were BM-MSCs. Furthermore, the osteogenic and adipogenic differentiation potential of these cells after induction were confirmed by ALP and Oil Red O staining. Notably, cells isolated from AIS patients showed weakened ALP staining, indicating impaired osteogenic differentiation potential of these cells (Supplementary Fig. 2).

Differential MiRNA expression

An unsupervised hierarchical clustering of the microarray data (Fig. 1) revealed significant miRNA expression changes (random-variance model *t* test p<.05 and FDR p<.05) in 54 miRNAs in AIS MSCs, as compared to controls. Among these 54 miRNAs, 42 were upregulated (such as miR-17-5p,

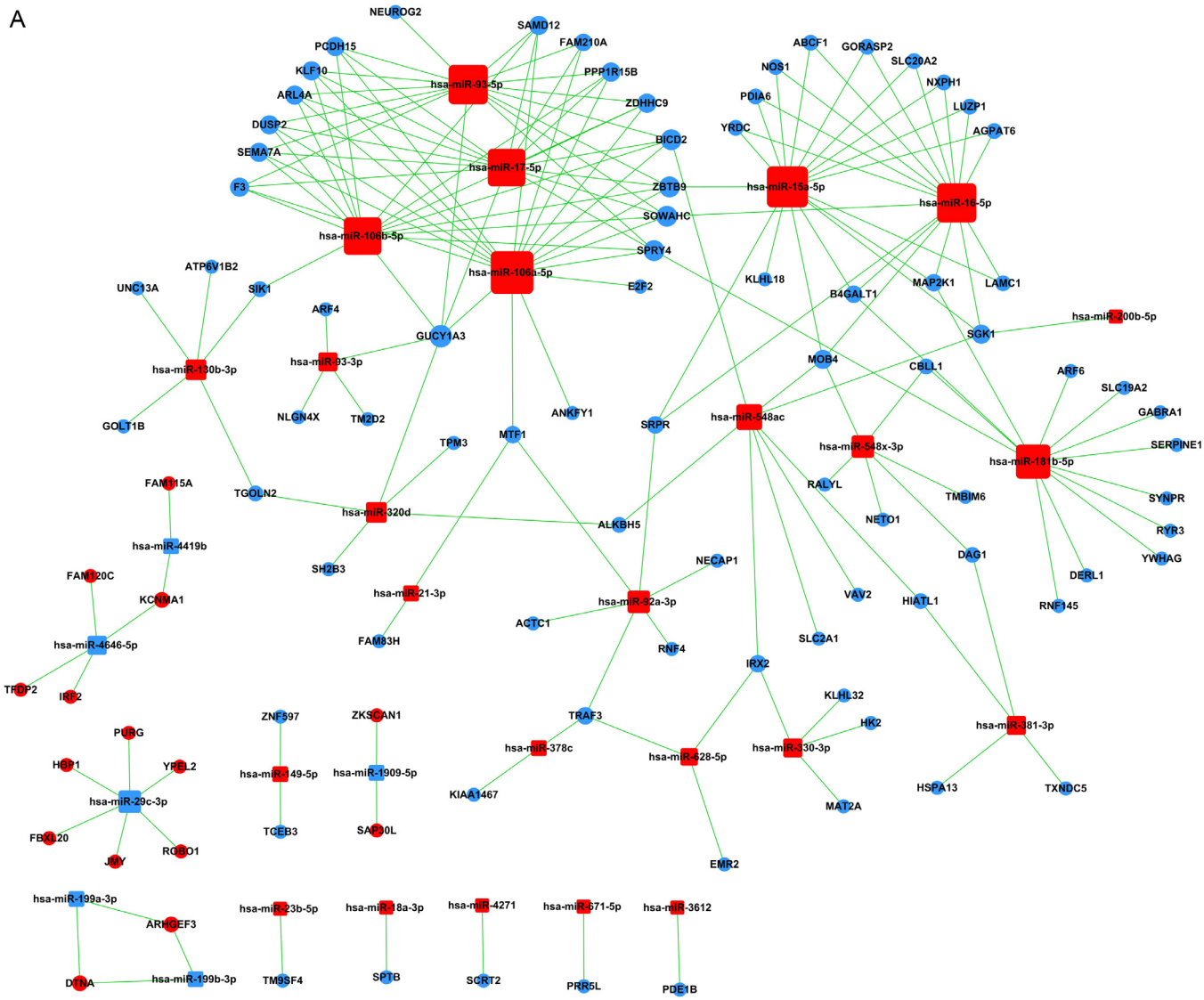

Fig. 4. (A) miRNA target gene network, (B) miRNA target GO network, and (C) miRNA target pathway network. Red cycle nodes represent upregulated genes, and blue cycle nodes represent downregulated genes. The nodes in the network were connected when their relations to target inhibiting in the interaction network. miRNAs with higher degrees are more centralized in the network and have a stronger capacity of modulating adjacent genes.

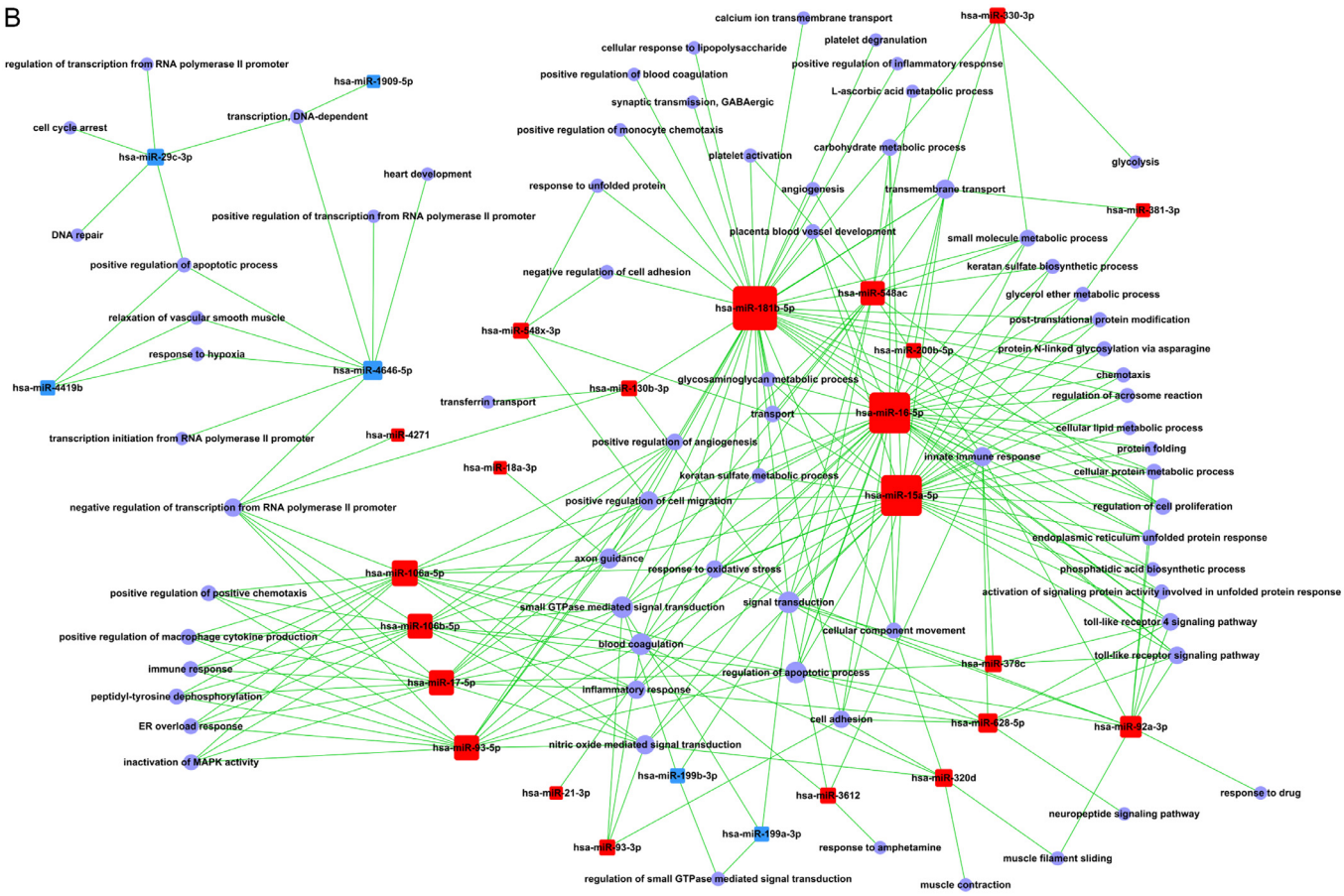

Fig. 4. Continued

miR-106a-5p, miR-106b-5p, miR-16-5p) and 12 were downregulated (such as miR-199a-3p, miR-29c-3p, miR-146b-3p, miR-126-3p; Supplementary Table 1).

GO analysis and pathway analysis based on MiRNAs

Authors searched for potential target genes of differentially expressed miRNAs using bioinformatic algorithms including MiRanda and TargetScan (Supplementary Table 2). According to the GO or KEGG database, we gained functions or pathways of all the target genes of differentially expressed miRNAs. And then, Fisher's exact test and v^2 test were used to calculate p value and FDR of all the target genes. According to the standard of $p<.05$, significant functions and pathways were filtered.

GO analysis

In our study, the main GO categories for upregulated miRNAs were related to functions such as small molecule metabolic process, transmembrane transport, immune response, etc. The main GO categories for downregulated miRNAs were related to functions such as small GTPase-mediated signal transduction, DNA-dependent transcription, cytokinesis, completion of separation, etc. (Fig. 2).

Pathways analysis

Biological pathway analyses generated significantly upregulated pathways and downregulated pathways. Among them, calcium signaling pathway, ubiquitin-mediated proteolysis, and Notch signaling pathway were upregulated, while MAPK signaling pathway, and phosphatidylinositol-3 kinase (PI3K)-Akt signaling pathway were downregulated (Fig. 3).

MiRNAs network analysis

MiRNA target gene (Fig. 4**A**), miRNA target GO (Fig. 4B), and miRNA target pathway analysis (Fig. 4C) were constructed. Venn diagram of the overlap top 10 miRNAs with the highest degree (**Tables 3–5**) from the three networks (Supplementary Table 3) revealed seven most significant central miRNAs (miR-17-5p, miR-106a-5p, miR-106b-5p, miR-16-5p, miR-93a-5p, miR-15a-5p, and miR-181b-5p; Fig. 5).

Extended sample validation of microarray data by qRT-PCR analysis

In order to independently confirm our microarray results, we enrolled another 30 AIS patients and 20 controls as the

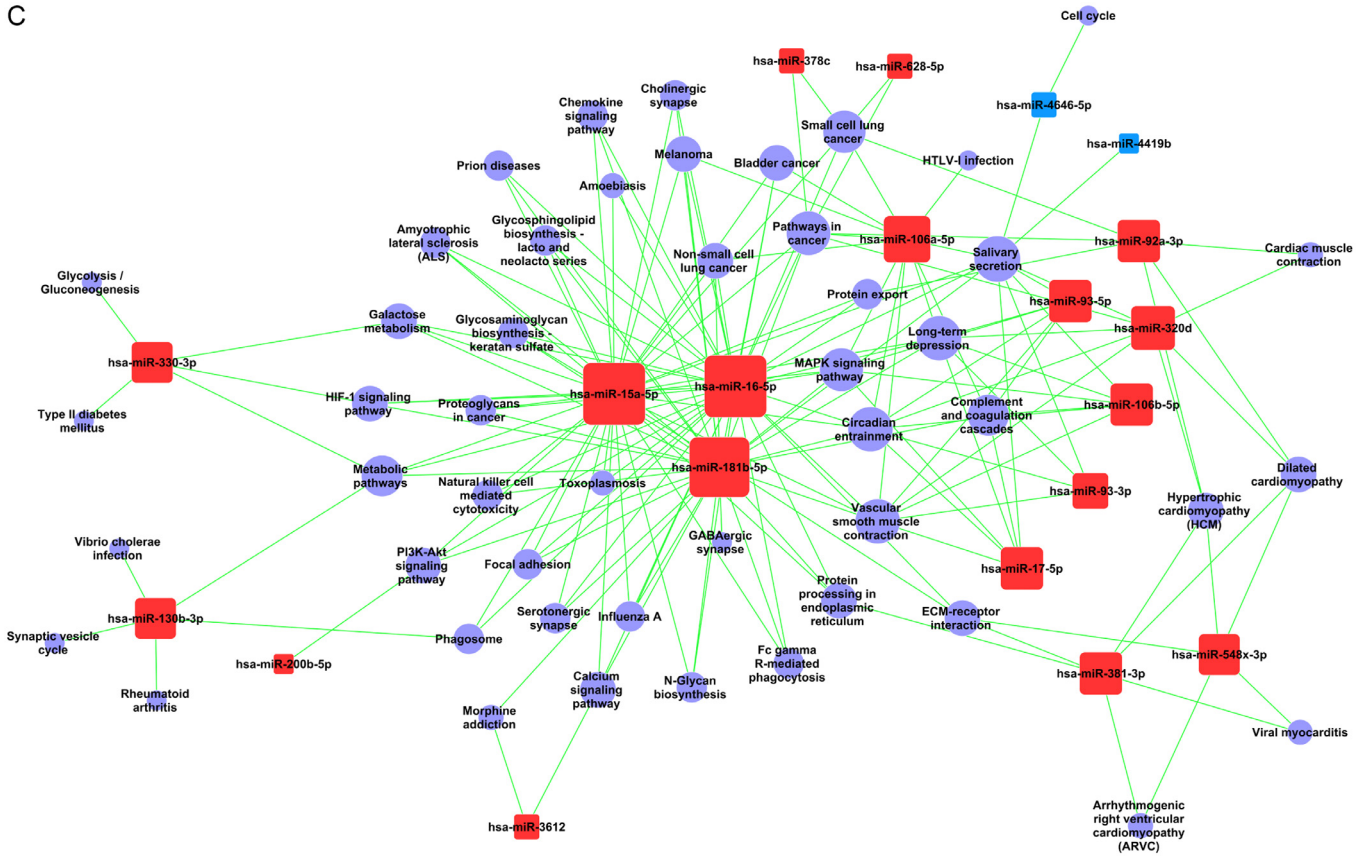

Fig. 4. Continued

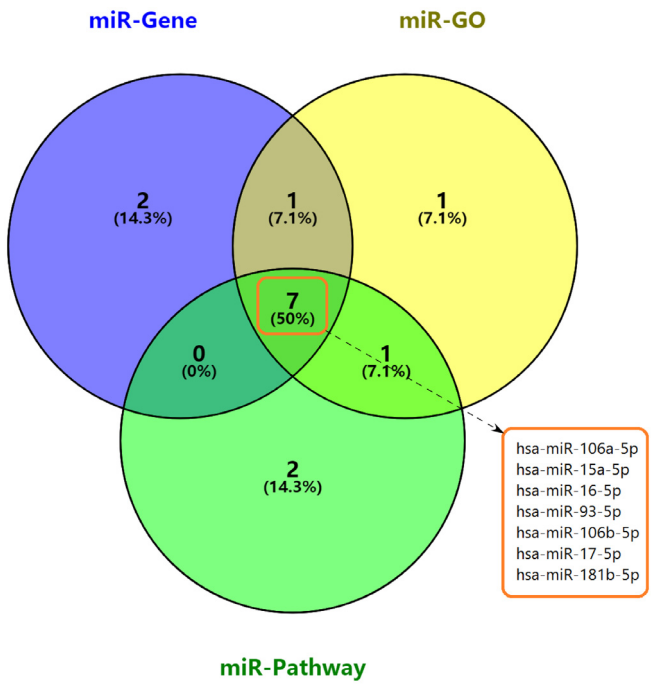

Fig. 5. Venn diagram of the overlap top 10 miRNAs from the three networks in Fig. 4.

extended sample to detect the expression level of 7 potentially crucial miRNAs using real-time quantitative PCR. As shown in Fig. 6, the changes in the expression levels of seven miRNAs were paralleled in microarray and qRT-PCR experiments, thereby confirming the reliability and validity of our findings and conclusions.

Target genes of differentially expressed miRNAs matched with dysregulated genes of AIS-MSCs

In our previous study, 1027 differentially expressed genes of MSCs from AIS patients were identified [11]. Therefore, the predicted target genes of differential expressed miRNAs in the present study were matched with these previously recognized dysregulated genes. A total of 204 target genes, including MAP2K1, SMAD3, GTF2I, CREBBP, and DUSP2 had been found as differential expressed genes in our previous research, which indicated that these miRNAs and their related genes worth further concern and analysis (Supplementary Table 4).

Discussion

To the best of our knowledge, this is the first miRNA microarray study in MSCs from AIS patients. Using

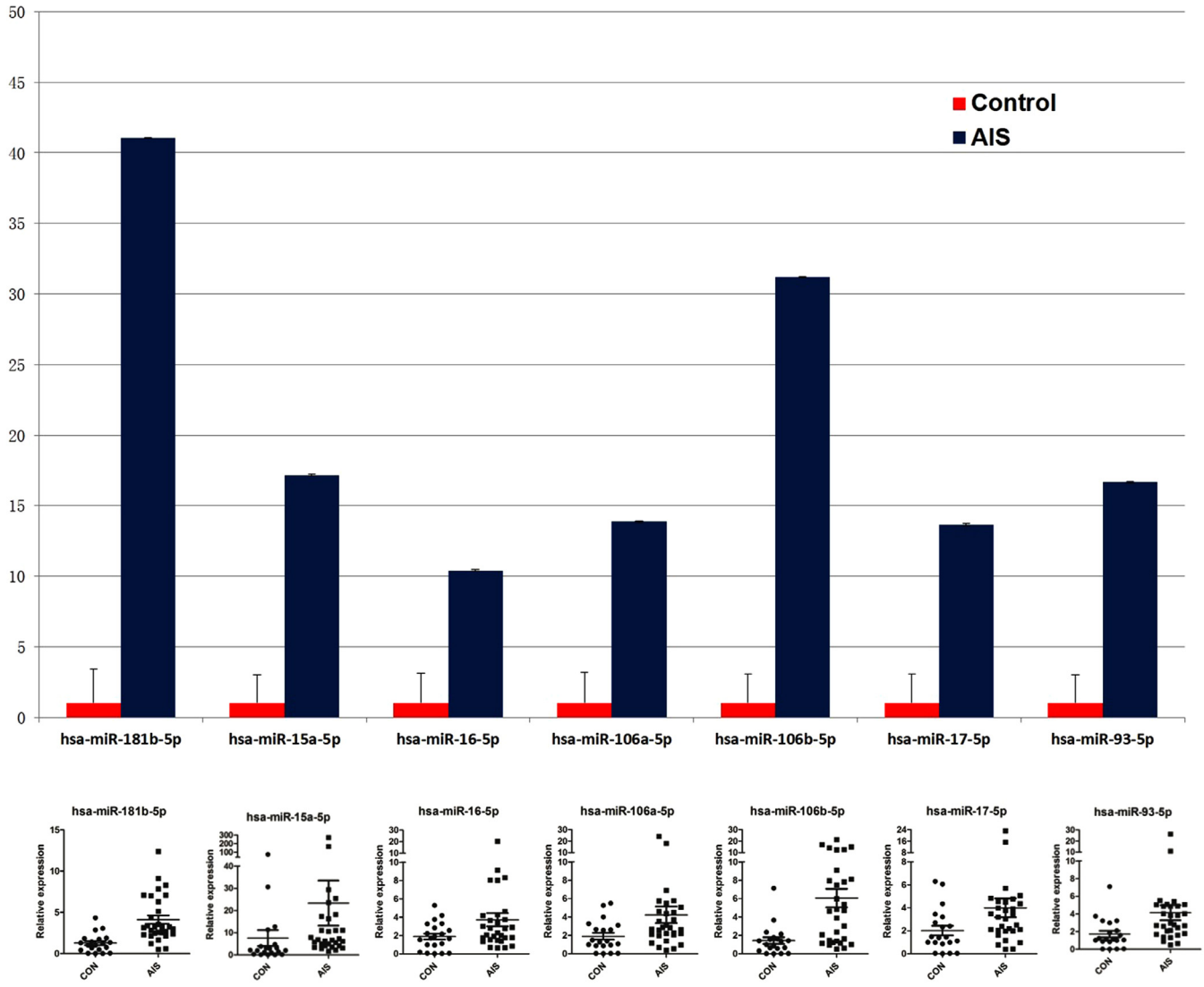

Fig. 6. Extended sample validation of microarray data by qRT-PCR analysis: Validation of 7 most significant central miRNAs according to Venn diagram analysis using RT-qPCR in 30 AIS patients and 20 controls. The relative level of mRNA of regulated genes was analyzed by quantitative RT-PCR. Gene expression results are depicted as $2^{-\Delta\Delta Ct}$ values, normalized to GAPDH. *p<.05, Student's *t* test, AIS (black) vs. control (white) expression levels.

microarray assay and integrated gene network analysis, 54 unreported miRNAs (12 upregulated, 42 downregulated) were identified as differentially expressed in MSCs from AIS patients compared with non-AIS patients for the first time. These miRNAs are involved in multiple biological processes, including signal transduction, small GTPase-mediated signal transduction, DNA-dependent transcription, cytokinesis, cell adhesion, transmembrane transport, response to hypoxia, etc. Pathway analysis of these new identified miRNAs revealed dysregulated MAPK signaling pathway, PI3K-Akt signaling pathway, calcium signaling pathway, Notch signaling pathway, and ubiquitin-mediated proteolysis pathway, all of which have been not only reported to play important role in regulating the osteogenic or adipogenic differentiation of MSCs [17–19]. The combinative GO and pathway enrichment analyses of these miRNAs have provided novel insight into the regulation of AIS genetic pathogenesis.

MAPK signaling pathway

Mitogen-activated protein kinases (MAPK) signaling pathway consists of four distinct cascades, including the extracellular signal-related kinases (ERK1/2), Jun amino-terminal kinases (JNK1/2/3), p38-MAPK, and ERK5 [20]. Previous studies have shown that MAPK pathway is one of the central signaling pathways involved in the induction of osteogenic differentiation of MSCs and regulation of bone formation [21,22].

Table 3
Top 10 miRNAs in MiRNA target gene network

Top 10 Mi-RNAs	Style	Degree
hsa-miR-106a-5p	up	18
hsa-miR-15a-5p	up	17
hsa-miR-16-5p	up	16
hsa-miR-93-5p	up	16
hsa-miR-106b-5p	up	15
hsa-miR-17-5p	up	15
hsa-miR-181b-5p	up	13
hsa-miR-548ac	up	8
hsa-miR-29c-3p	down	6
hsa-miR-548x-3p	up	6

Table 4
Top 10 miRNAs in miRNA target pathway network

Top 10 Mi-RNAs	Style	Degree
hsa-miR-15a-5p	up	34
hsa-miR-16-5p	up	34
hsa-miR-181b-5p	up	31
hsa-miR-106a-5p	up	12
hsa-miR-320d	up	8
hsa-miR-106b-5p	up	6
hsa-miR-17-5p	up	6
hsa-miR-381-3p	up	6
hsa-miR-92a-3p	up	6
hsa-miR-93-5p	up	6

Table 5
Top 10 miRNAs in miRNA target GO network

Top 10 Mi-RNAs	Style	Degree
hsa-miR-181b-5p	up	38
hsa-miR-15a-5p	up	34
hsa-miR-16-5p	up	34
hsa-miR-106a-5p	up	16
hsa-miR-106b-5p	up	15
hsa-miR-17-5p	up	15
hsa-miR-93-5p	up	15
hsa-miR-548ac	up	14
hsa-miR-92a-3p	up	11
hsa-miR-4646-5p	down	8

MAPK/ERK signaling activated by MAP2K1 can induce osteoblast gene expression, while inhibition of MAPK signaling intermediately blocked differentiation [23]. In addition, NEL-like protein 1 (NELL-1) activates both ERK1/2 and JNK1 MAPK pathways in osteosarcoma cell type, resulting in Runt related-transcription factor 2 (Runx2) protein phosphorylation [24]. Furthermore, overexpression of miR-214 could downregulate the osteogenic differentiation of BMSCs by inhibiting the JNK and p38 MAPK pathways [25]. Our previous study has reported a dysregulated MAPK signaling pathway in pathway analysis according to differentially expressed genes in MSCs from AIS patients [11]. In this present study, we further proved that the MAPK signaling pathway was downregulated in MSCs from AIS patients using pathway analysis of differential miRNAs. Taken together, these data strongly suggest that downregulated MAPK pathway plays a significant role in the abnormal bone formation in AIS patients.

PI3K/Akt signaling pathway

Phosphoinositide 3-kinase (PI3K)/Akt pathway plays a crucial role in regulating cell proliferation, apoptosis, differentiation, and migration [26]. Numerous studies have shown that the PI3K/Akt signaling pathway is essential for MSC osteogenesis. In human MSCs, knockdown of Caveolin-1 expression and cholesterol oxidase treatment enhanced Akt activation in response to osteogenic supplements [27]. In mice, knockout of Akt negatively affected murine endochondral ossification [28,29]. Furthermore, longitudinal bone growth in mouse embryonic tibiae was suppressed by inhibition of PI3K/Akt signaling [30]. In addition, in MC3T3-E1 cells and diabetic mouse model, miR-378 activated the PI3K/Akt signaling pathway by targeting caspase-3 (CASP3), which could attenuate high glucose-suppressed osteogenic differentiation [31]. Both our previous differential genetic results of AIS-MSCs [11] and the present study indicate that PI3K/Akt signaling pathway is significantly downregulated in MSCs from AIS patients. Collectively, these results suggest that PI3K/Akt signaling pathway may play an important role in bone formation and maturation in AIS patients.

Furthermore, our signal network analysis of differential expressed miRNAs involved in significant pathways could construct the interaction network from differential miRNAs and could find the central miRNAs with the highest degree. In this study, seven potentially crucial miRNAs, including miR-17-5p, miR-106a-5p, miR-106b-5p, miR-16-5p, miR-93-5p, miR-15a-5p, and miR-181b-5p were selected for validation considering both their positions in the network and potential biological functions, which may play essential roles in AIS pathogenesis and accompanied abnormal bone metabolism. We summarize the sequence, miRNA accession, previously reported possible functions, and related references of these seven potentially crucial miRNAs in Table 6.

Furthermore, in our previous study, 1027 differentially expressed genes of MSCs from AIS patients were identified [11]. Interestingly, the predicted target genes of differential expressed miRNAs in present study are partially matched with previously recognized dysregulated genes of AIS MSCs, such as MAP2K1, SMAD3, GTF2I, CREBBP, and DUSP2, implying the crucial role of these target genes and their related miRNAs in AIS pathogenesis, which also required further concern and analysis.

Our study has possible limitations. First, our microarray results are based on 10 AIS patients and 5 age- and gender-matched non-AIS patients, which is a relatively small

Table 6
Characteristics of seven potentially crucial miRNAs

miRNA	Sequence	miRNA_Acc*	Previously reported possible function	Ref.
miR-17-5p	CAAAGUGCUUA-CAGUGCAGGUAG	MIMAT0000070	A member of miR-17 family, deriving from miR-17-92 cluster and its two paralogues	[32]
			Upregulated miR-17-5p expression inhibited osteogenesis, whereas promoted adipogenic differentiation in human adipose-derived mesenchymal stem cells (hADSCs) and other cell lines	[33,34]
			Silencing of miR-17-5p promoted bone formation in vivo	[33]
			By targeting either Smad5 or SMAD7, miR-17-5p functioned as a crucial factor in different pathways, including TGF-β pathway and β-catenin dependent/independent Wnt pathway, which regulated osteogenic differentiation of MSCs	[33,35,36]
			miR-17-5p was obviously downregulated during the process of osteogenic differentiation	[33]
			By targeting Smad5, miR-17-5p could suppress osteogenic differentiation and regulate bone formation in vivo	[33]
miR-106a/b	AAAAGUGCUUACA-GUGCAGGUAG/ UAAAGUGCUGA-CAGUGCAGAU	MIMAT0000103/ MIMAT0000680	Members of miR-17 family were both upregulated in AIS MSCs according to our results	[32]
			The specific expression of miR-106a exists during hMSCs differentiation toward osteoblasts	[37]
			miR-106a regulated osteogenic and adipogenic differentiation of hADSCs by directly targeting bone morphogenetic protein 2 (BMP2), resulting in downregulation of osteogenic gene TAZ, MSX2 and Runx2, and upregulation of adipogenic gene C/EBPα and PPARγ	[34]
			miR-106b-5p was obviously downregulated during the process of osteogenic differentiation	[33]
			By targeting Smad5, miR-106b-5p could suppress osteogenic differentiation and regulate bone formation in vivo	[33]
			In vitro and in the glucocorticoid-induced osteoporosis (GIOP) mouse model, miR-106b inhibited osteoblastic differentiation and bone formation, partly by directly targeting BMP2	[38]
miR-16-5p	UAGCAGCACGU-AAAUAUUGGCG	MIMAT0000069	Several studies reported the role of miR-16-5p in the development of osteoarthritis and RANKL-induced osteoclast formation	[39,40]
			By regulating SMAD3 expression, miR-16-5p played an important role in TGF-β pathway, which was involved in chondrocyte cell growth and differentiation during chondrogenesis	[39]
			In giant cell tumor, miR-16-5p expression considerably decreased with the progression of receptor activator of nuclear factor-κB ligand- (RANKL-) induced osteoclastogenesis, while miR-16-5p mimics significantly reduced RANKL-induced osteoclast formation	[40]
miR-93-5p	CAAAGUGCUGUU-CGUGCAGGUAG	MIMAT0000093	By directly targeting Smad5, miR-93-5p could suppress osteogenic differentiation of C3H10T1/2 cells	[41]
			miR-93-5p has inhibitory effect on osteogenic differentiation of hBMSCs by targeting BMP-2	[42]
			Enhanced cell proliferation of hBMSCs during in vitro experiments was also observed, which indicated that miR-93-5p may have multiple regulatory roles during hBMSCs differentiation and bone formation	[42]
miR-15a-5p	UAGCAGCACAUAA-UGGUUUGUG	MIMAT0000068	Abnormal overexpression of miR-15a-5p was reported to suppress cancer proliferation, induce cell cycle arrest in human hepatocellular carcinoma cells, and have a specific and negative regulating effect on brain-derived neurotrophic factor (BDNF)	[43]
			Overexpression of miR-15a-5p contributed to cell apoptosis and matrix degradation via inhibiting vascular endothelial growth factor A (VEGFA), resulting in osteoarthritis (OA) progression and inhibiting apoptosis of OA chondrocytes	[44]
miR-181b-5p	AACAUUCAUUGCU-GUCGGUGGGU	MIMAT0000257	During mouse calvarial and tibial development, miR-181a promoted osteoblastic differentiation via repression of TGF-β signaling molecules, implying the potential role in both endochondral and intramembranous ossification	[45]

* **miRNA_Acc: miRNA accession.**

sample size. Although we had performed extended sample validation of microarray data by qRT-PCR analysis in 30 AIS patients and 20 controls with satisfying parallel results, our findings still require further validation of future studies with larger samples. Second, the participants in this study were from our single center. Although they are from several different races and different geographic provinces in the same country, the racial distribution is far from large enough to cover the overall population. Therefore, our findings should be considered with this concern and require further validation studies from other institutions in other parts of the world.

In summary, the current study reports the differential miRNAs expression profiles of BM-MSCs from AIS patients and related pathways for the first time. The identification of these candidate miRNAs provides a deep insight into the pathogenesis of AIS and the accompanying generalized osteopenia.

Acknowledgments

This work was supported by the National Natural Science Foundation of China (81272054, 81171673), Beijing Talent Fund (2015000021223ZK27), Beijing Nova program Grant (2014A019), Beijing High-level Innovative Entrepreneurial Talent Fund, Peking Union Medical College Youth Fund, PUMC Nova program Grant of Chinese academy of medical sciences. The authors declare that they have no conflict of interests related to this work.

Supplementary materials

Supplementary material associated with this article can be found in the online version at https://doi.org/10.1016/j.spinee.2019.05.003.

References

[1] Yim AP, Yeung HY, Hung VW, et al. Abnormal skeletal growth patterns in adolescent idiopathic scoliosis—a longitudinal study until skeletal maturity. Spine (Phila Pa 1976) 2012;37:E1148–54.
[2] Barrios C, Cortes S, Perez-Encinas C, et al. Anthropometry and body composition profile of girls with nonsurgically treated adolescent idiopathic scoliosis. Spine (Phila Pa 1976) 2011;36:1470–7.
[3] Wei-Jun W, Xu S, Zhi-Wei W, Xu-Sheng Q, Zhen L, Yong Q. Abnormal anthropometric measurements and growth pattern in male adolescent idiopathic scoliosis. Eur Spine J 2012;21:77–83.
[4] Song XX, Jin LY, Li XF, et al. Effects of low bone mineral status on biomechanical characteristics in idiopathic scoliotic spinal deformity. World Neurosurg 2018;110:e321–9.
[5] Akazawa T, Kotani T, Sakuma T, et al. Bone mineral density and physical performance of female patients 27 years or longer after surgery for adolescent idiopathic scoliosis. Asian Spine J 2017;11:780–6.
[6] Yip BH, Yu FW, Wang Z, et al. Prognostic value of bone mineral density on curve progression: a longitudinal cohort study of 513 girls with adolescent idiopathic scoliosis. Sci Rep 2016;6:39220.
[7] Bao H, Liu Z, Yan P, Qiu Y, Zhu F. Disproportionate growth between the spine and pelvis in patients with thoracic adolescent scoliosis: a new look into the pattern's growth. Bone Joint J 2015;97-B:1668–74.
[8] Ishida K, Aota Y, Mitsugi N, et al. Relationship between bone density and bone metabolism in adolescent idiopathic scoliosis. Scoliosis 2015;10:19.
[9] Park WW, Suh KT, Kim JI, Kim SJ, Lee JS. Decreased osteogenic differentiation of mesenchymal stem cells and reduced bone mineral density in patients with adolescent idiopathic scoliosis. Eur Spine J 2009;18:1920–6.
[10] Chen C, Xu C, Zhou T, et al. Abnormal osteogenic and chondrogenic differentiation of human mesenchymal stem cells from patients with adolescent idiopathic scoliosis in response to melatonin. Mol Med Rep 2016;14:1201–9.
[11] Zhuang Q, Mao W, Xu P, et al. Identification of differential genes expression profiles and pathways of bone marrow mesenchymal stem cells of adolescent idiopathic scoliosis patients by microarray and integrated gene network analysis. Spine (Phila Pa 1976) 2016;41:840–55.
[12] Wang Q, Yang J, Lin X, Huang Z, Xie C, Fan H. Spot14/Spot14R expression may be involved in MSC adipogenic differentiation in patients with adolescent idiopathic scoliosis. Mol Med Rep 2016;13:4636–42.
[13] Yan Z, Guo Y, Wang Y, Li Y, Wang J. MicroRNA profiles of BMSCs induced into osteoblasts with osteoinductive medium. Exp Ther Med 2018;15:2589–96.
[14] Tang J, Zhang Z, Jin X, Shi H. miR-383 negatively regulates osteoblastic differentiation of bone marrow mesenchymal stem cells in rats by targeting Satb2. Bone 2018;114:137–43.
[15] Tang Y, Zhang L, Tu T, et al. MicroRNA-99a is a novel regulator of KDM6B-mediated osteogenic differentiation of BMSCs. J Cell Mol Med 2018;22:2162–76.
[16] Zhuang Q, Li J, Wu Z, et al. Differential proteome analysis of bone marrow mesenchymal stem cells from adolescent idiopathic scoliosis patients. PLoS One 2011;6:e18834.
[17] Chen J, Crawford R, Chen C, Xiao Y. The key regulatory roles of the PI3K/Akt signaling pathway in the functionalities of mesenchymal stem cells and applications in tissue regeneration. Tissue Eng Part B Rev 2013;19:516–28.
[18] James AW. Review of signaling pathways governing MSC osteogenic and adipogenic differentiation. Scientifica (Cairo) 2013;2013:684736.
[19] Yuan Z, Li Q, Luo S, et al. PPARgamma and Wnt signaling in adipogenic and osteogenic differentiation of mesenchymal stem cells. Curr Stem Cell Res Ther 2016;11:216–25.
[20] Sun Y, Liu WZ, Liu T, et al. Signaling pathway of MAPK/ERK in cell proliferation, differentiation, migration, senescence and apoptosis. J Recept Signal Transduct Res 2015;35:600–4.
[21] Kanno T, Takahashi T, Tsujisawa T, Ariyoshi W, Nishihara T. Mechanical stress-mediated Runx2 activation is dependent on Ras/ERK1/2 MAPK signaling in osteoblasts. J Cell Biochem 2007;101:1266–77.
[22] Ge C, Xiao G, Jiang D, Franceschi RT. Critical role of the extracellular signal-regulated kinase-MAPK pathway in osteoblast differentiation and skeletal development. J Cell Biol 2007;176:709–18.
[23] Franceschi RT, Ge C, Xiao G, Roca H, Jiang D. Transcriptional regulation of osteoblasts. Ann N Y Acad Sci 2007;1116:196–207.
[24] Chen F, Walder B, James AW, et al. NELL-1-dependent mineralisation of Saos-2 human osteosarcoma cells is mediated via c-Jun N-terminal kinase pathway activation. Int Orthop 2012;36:2181–7.
[25] Guo Y, Li L, Gao J, Chen X, Sang Q. miR-214 suppresses the osteogenic differentiation of bone marrow-derived mesenchymal stem cells and these effects are mediated through the inhibition of the JNK and p38 pathways. Int J Mol Med 2017;39:71–80.
[26] Chen J. Multiple signal pathways in obesity-associated cancer. Obes Rev 2011;12:1063–70.
[27] Baker N, Sohn J, Tuan RS. Promotion of human mesenchymal stem cell osteogenesis by PI3-kinase/Akt signaling, and the influence of caveolin-1/cholesterol homeostasis. Stem Cell Res Ther 2015;6:238.

[28] Peng XD, Xu PZ, Chen ML, et al. Dwarfism, impaired skin development, skeletal muscle atrophy, delayed bone development, and impeded adipogenesis in mice lacking Akt1 and Akt2. Genes Dev 2003;17:1352–65.
[29] Ulici V, Hoenselaar KD, Agoston H, et al. The role of Akt1 in terminal stages of endochondral bone formation: angiogenesis and ossification. Bone 2009;45:1133–45.
[30] Ulici V, Hoenselaar KD, Gillespie JR, Beier F. The PI3K pathway regulates endochondral bone growth through control of hypertrophic chondrocyte differentiation. BMC Dev Biol 2008;8:40.
[31] You L, Gu W, Chen L, Pan L, Chen J, Peng Y. MiR-378 overexpression attenuates high glucose-suppressed osteogenic differentiation through targeting CASP3 and activating PI3K/Akt signaling pathway. Int J Clin Exp Pathol 2014;7:7249–61.
[32] Mendell JT. miRiad roles for the miR-17-92 cluster in development and disease. Cell 2008;133:217–22.
[33] Fang T, Wu Q, Zhou L, Mu S, Fu Q. miR-106b-5p and miR-17-5p suppress osteogenic differentiation by targeting Smad5 and inhibit bone formation. Exp Cell Res 2016;347:74–82.
[34] Li H, Li T, Wang S, et al. miR-17-5p and miR-106a are involved in the balance between osteogenic and adipogenic differentiation of adipose-derived mesenchymal stem cells. Stem Cell Res 2013;10:313–24.
[35] Chen G, Deng C, Li YP. TGF-beta and BMP signaling in osteoblast differentiation and bone formation. Int J Biol Sci 2012;8:272–88.
[36] Jia J, Feng X, Xu W, et al. MiR-17-5p modulates osteoblastic differentiation and cell proliferation by targeting SMAD7 in non-traumatic osteonecrosis. Exp Mol Med 2014;46:e107.
[37] Vimalraj S, Selvamurugan N. MicroRNAs expression and their regulatory networks during mesenchymal stem cells differentiation toward osteoblasts. Int J Biol Macromol 2014;66:194–202.
[38] Liu K, Jing Y, Zhang W, et al. Silencing miR-106b accelerates osteogenesis of mesenchymal stem cells and rescues against glucocorticoid-induced osteoporosis by targeting BMP2. Bone 2017;97:130–8.
[39] Li L, Jia J, Liu X, et al. MicroRNA-16-5p controls development of osteoarthritis by targeting SMAD3 in chondrocytes. Curr Pharm Des 2015;21:5160–7.
[40] Sang S, Zhang Z, Qin S, Li C, Dong Y. MicroRNA-16-5p inhibits osteoclastogenesis in giant cell tumor of bone. Biomed Res Int 2017;2017:3173547.
[41] Xu L, Li X, Liu Y, Kong Q, Long D, Li S. miR-93-5P suppresses osteogenic differentiation of mouse C3H10T1/2 CELLS BY targeting Smad5. Zhongguo Xiu Fu Chong Jian Wai Ke Za Zhi 2015;29:1288–94.
[42] Zhang Y, Wei QS, Ding WB, et al. Increased microRNA-93-5p inhibits osteogenic differentiation by targeting bone morphogenetic protein-2. PLoS One 2017;12:e0182678.
[43] Long J, Jiang C, Liu B, Fang S, Kuang M. MicroRNA-15a-5p suppresses cancer proliferation and division in human hepatocellular carcinoma by targeting BDNF. Tumour Biol 2016;37:5821–8.
[44] Chen H, Tian Y. MiR-15a-5p regulates viability and matrix degradation of human osteoarthritis chondrocytes via targeting VEGFA. Biosci Trends 2017;10:482–8.
[45] Bhushan R, Grunhagen J, Becker J, Robinson PN, Ott CE, Knaus P. miR-181a promotes osteoblastic differentiation through repression of TGF-beta signaling molecules. Int J Biochem Cell Biol 2013;45:696–705.